

International Journal of Statistics and Applied Mathematics



ISSN: 2456-1452
NAAS Rating (2026): 4.49
Maths 2026; 11(1): 01-07
© 2026 Stats & Maths
<https://www.mathsjournal.com>
Received: 02-10-2025
Accepted: 06-11-2025

T Gangaram
Lecturer, Department of Statistics, SVA Government College, Srikalahasti, Andhra Pradesh, India

V Munaiah
Lecturer, Department of Statistics, SVA Government College, Srikalahasti, Andhra Pradesh, India

G SatyanarayanaReddy
Lecturer, Department of Statistics, Government College for Men (A), Kadapa, Andhra Pradesh, India

J Kishore Kumar
Associate Professor, Department of Statistics, Maharani Science College for Women, Bangalore, Karnataka, India

Corresponding Author:
T Gangaram
Lecturer, Department of Statistics, SVA Government College, Srikalahasti, Andhra Pradesh, India

Significance of non-Fourier heat flux on the maxwell fluid flow over an inclined vertical plate: A multiple linear regression analysis

T Gangaram, V Munaiah, G SatyanarayanaReddy and J Kishore Kumar

DOI: <https://www.doi.org/10.22271/math.2026.v11.i1a.2233>

Abstract

This study numerically investigates the significance of non-Fourier heat conduction on the magnetohydrodynamic (MHD) flow of a Maxwell fluid over an inclined vertical plate, incorporating the effects of thermal radiation and couple stresses. The Cattaneo-Christov heat flux model is employed to account for finite thermal relaxation time, moving beyond the classical Fourier's law. The governing equations are transformed into a system of ordinary differential equations and solved using the bvp4c solver in MATLAB. The results indicate that the fluid velocity declines with increasing Weissenberg and couple stress parameters, while the temperature profile is enhanced by thermal radiation but diminished by the thermal relaxation parameter. Furthermore, a multiple linear regression analysis yields predictive models, revealing that the skin friction coefficient increases with the magnetic field and couple stress parameters, and the Nusselt number is augmented by the Prandtl number and thermal radiation.

Keywords: Cattaneo-Christov heat flux, maxwell fluid, multiple linear regression, thermal radiation, MHD

Introduction

Heat transmission and temperature distribution in a fluid's boundary layer flow can be dramatically impacted by thermal radiation at high temperatures. Radiative flows of a hot, electrically conducting fluid near a magnetic field are used in many different types of industries, including but not limited to electrical power generation, nuclear engineering applications, solar power technologies, and others. Kumar *et al.* [1] numerically investigated MHD natural convective nanofluid flow over a vertical plate under thermal radiation using the finite element method. It is found that the velocity and temperature profiles increase with higher radiation parameter but decrease with stronger magnetic field. Sankad *et al.* [2] analysed MHD boundary layer flow of a Casson nanofluid containing gyrotactic microorganisms over a stretching sheet, considering thermal radiation and variable wall temperature using the Differential Transform Method. It is noticed that the fluid velocity decreases with increasing and Casson parameter, while temperature rises with higher thermophoresis parameter. Kumar *et al.* [3] numerically analysed MHD Casson fluid flow over a stretching surface with nonlinear thermal radiation, chemical reaction, and heat generation/absorption using the RK-based shooting method. It is observed that the fluid concentration decreases with higher chemical reaction and Schmidt numbers. Shah *et al.* [4] numerically analysed MHD Carreau fluid flow over a nonlinear stretching/shrinking surface with thermal radiation, chemical reaction, and temperature-dependent thermophysical properties using a shooting method. Shankar Goud and Mahantesh [5] numerically investigated the effect of thermal radiation on MHD heat transfer in a micropolar fluid over a vertical moving porous plate using the Galerkin finite element method. After that, a number of scholars [6-10] addressed the impact of the same parameter (thermal radiation) on a variety of fluid flows across a range of different geometries. The Cattaneo-Christov (C-C) heat flux model, which builds on Fourier's law, includes a finite thermal relaxation period to show that heat transmission happens at a finite speed.

Adding the C-C heat flow to the governing equations might help engineers make better guesses about how non-Newtonian fluids will behave when they are heated. This is useful in areas like polymer production and biofluid mechanics. Hayat *et al.* [11] investigated the magnetohydrodynamic flow of a fourth-grade nanofluid over a stretching surface embedded in a Darcy-Forchheimer porous medium, incorporating melting heat transfer and Cattaneo-Christov heat flux. The governing equations were solved using the optimal homotopy analysis method (OHAM) under relevant boundary conditions. Tassaddiq [12] analysed the magnetohydrodynamic flow and heat transfer of a hybrid nano-micropolar fluid over a stretching surface using the Cattaneo-Christov heat flux model, considering viscous and Joule dissipation effects. The problem was solved using both analytical (Homotopy Analysis Method) and numerical (Shooting Method) approaches. Rao *et al.* [13] numerically investigated the non-Darcy flow of a Cross fluid past a tilted plate, incorporating the Cattaneo-Christov heat flux model, thermal radiation, chemical reaction, and cross-diffusion (Soret and Dufour) effects. Chandra Sekar Reddy *et al.* [14] investigated the magnetohydrodynamic flow and heat transfer of an Ag-SWCNT/water Maxwell hybrid nanofluid over a vertical cone using the Cattaneo-Christov heat flux model, incorporating thermal radiation, chemical reaction, and convective boundary conditions. The governing equations were solved numerically using the finite element method. Rehman *et al.* [15] studied the flow of a third-grade fluid over a stretching surface using the Cattaneo-Christov heat flux model and incorporating Soret-Dufour effects under magnetohydrodynamic (MHD) conditions. After that, a number of scholars [16-20] addressed a variety of fluid flows across a range of different geometries using Cattaneo-Christov heat flux model.

The novelty of the present work lies in the comprehensive analysis of a non-Newtonian Maxwell fluid flow over an inclined vertical plate by integrating the Cattaneo-Christov non-Fourier heat flux model with thermal radiation and magnetic field effects, followed by the development of predictive multiple linear regression models for key engineering parameters. This approach not only provides deeper insight into the complex thermal and hydrodynamic boundary layer behaviour but also bridges the gap between theoretical analysis and practical application. The findings have significant applications in enhancing the design and thermal management of advanced industrial systems, such as polymer processing equipment, nuclear reactor cooling, solar energy collectors, and aerodynamic heating in high-speed flight, where accurate prediction of heat transfer and skin friction under radiative and magnetic influences is crucial.

Mathematical Formulation

The flow is assumed to be steady, laminar, and two-dimensional, occurring over an inclined vertical plate. A uniform external magnetic field of strength B is applied vertically (see Fig. 1), while the induced magnetic field is considered negligible due to a small magnetic Reynolds number. The fluid is modeled as a non-Newtonian Maxwell fluid, accounting for viscoelastic effects. Furthermore, the heat transfer mechanism incorporates the Cattaneo-Christov heat flux model to capture non-Fourier effects with a finite thermal relaxation time, and the influence of thermal radiation is also integrated into the energy equation.

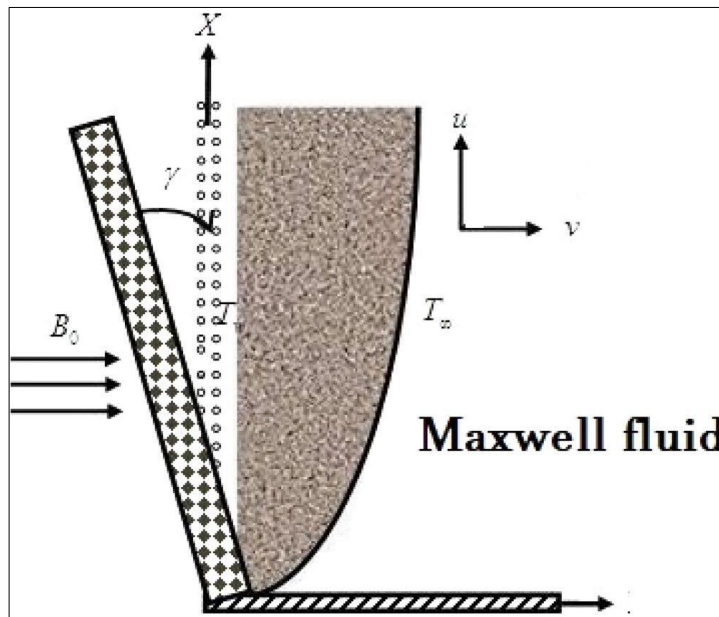


Fig 1: Schematic diagram

The following are the necessary conditions and equations for this study, based on the assumptions made above:

$$\frac{\partial v}{\partial y} + \frac{\partial u}{\partial x} = 0 \quad (1)$$

$$u \frac{\partial u}{\partial x} + v \frac{\partial u}{\partial y} = \frac{\mu}{\rho} \frac{\partial^2 u}{\partial y^2} - \kappa \left[\frac{\partial^2 u}{\partial x^2} u^2 + \frac{\partial^2 u}{\partial y^2} v^2 + 2v \frac{\partial^2 u}{\partial x \partial y} u \right] - \frac{\sigma}{\rho} B_0^2 u - \frac{\gamma_0}{\rho} \frac{\partial^4 u}{\partial y^4} + g \beta_T (T - T_\infty) \cos \gamma \quad (2)$$

$$u \frac{\partial T}{\partial x} + v \frac{\partial T}{\partial y} = \frac{k}{(\rho C_p)} \frac{\partial^2 T}{\partial y^2} - \Upsilon \left[\begin{array}{l} u^2 \frac{\partial^2 T}{\partial x^2} + u \frac{\partial u}{\partial x} \frac{\partial T}{\partial x} + v \frac{\partial u}{\partial y} \frac{\partial T}{\partial x} + 2uv \frac{\partial^2 T}{\partial x \partial y} \\ + u \frac{\partial v}{\partial x} \frac{\partial T}{\partial y} + v \frac{\partial v}{\partial y} \frac{\partial T}{\partial y} + v^2 \frac{\partial^2 T}{\partial y^2} \end{array} \right] \\ + \frac{1}{(\rho C_p)} \frac{16}{3} \frac{\sigma^* T_\infty^3}{k^*} \frac{\partial^2 T}{\partial y^2} \quad (3)$$

$$\left. \begin{array}{l} \text{at } y=0 : v=0, u=0, \frac{\partial^2 u}{\partial y^2}=0, T=T_w, \\ \text{as } y \rightarrow \infty : u \rightarrow 0, \frac{\partial u}{\partial y} \rightarrow 0, T \rightarrow T_\infty. \end{array} \right\} \quad (4)$$

For the purpose of converting regulatory equations, Sudarmozhi *et al.* [21] introduced further similarity transformations:

$$\left. \begin{array}{l} \eta = \frac{y}{x} Ra_x^{0.25}, Ra_x = \frac{g \beta_T (T_w - T_\infty) x^3}{\alpha \nu}, u = \frac{\alpha}{x} Ra_x^{0.5} f', \\ v = \frac{\alpha}{4x} \eta Ra_x^{0.25} f' - \frac{3\alpha}{4x} Ra_x^{0.25} f, T = T_\infty + \theta(\eta)(T_w - T_\infty). \end{array} \right\} \quad (5)$$

Through the use of terms in (5), the continuity equation (1) is satisfied in a straightforward manner. Terms in (5) can then be skilfully used to convert (2 - 3) as the following:

$$\left. \begin{array}{l} \left(-\frac{9}{16} We f^2 \right) f''' + \frac{3}{4} f f'' - \frac{f'^2}{2} - \sqrt{\Pr} (M) f' - We \left(\frac{3}{16} \eta f'^2 f'' - \frac{3}{8} f f' f'' - \frac{1}{4} f'^3 \right) \\ + \Pr(\theta) \cos \gamma - C s f^v = 0 \end{array} \right\} \quad (6)$$

$$\left. \begin{array}{l} \left(1 + \frac{4}{3} R - \frac{1}{\sqrt{\Pr}} \Gamma f^2 \right) \theta'' + \frac{3}{4} f \theta' - \frac{15}{16} \frac{\Gamma}{\sqrt{\Pr}} f f' \theta' = 0 \end{array} \right\} \quad (7)$$

$$\left. \begin{array}{l} \text{at } \eta=0 : f=0, f'=0, \theta=1, f'''=0, \\ \text{at } \eta \rightarrow \infty : \theta \rightarrow 0, f'' \rightarrow 0, f' \rightarrow 0. \end{array} \right\} \quad (8)$$

where

$$\Pr = \frac{\nu}{\alpha}, M = \sqrt{\frac{1}{g \beta_T (T_w - T_\infty)}} \frac{\sigma B^2}{\rho}, C s = \sqrt{\frac{g \beta_T (T_w - T_\infty)}{\nu}} \frac{\gamma_1}{\rho \alpha^{3/2}}, \\ \gamma_0 = \gamma_1 \sqrt{x}, R = \frac{4 \sigma^* T_\infty^3}{k k^*}, \kappa = \kappa_0 \sqrt{x}, \Gamma = \lambda_0 \sqrt{g \beta_T (T_w - T_\infty)}, \lambda_0 = \frac{\lambda}{\sqrt{x}}.$$

Friction factor, Nusselt and Sherwood numbers are outlined as:

$$\left. \begin{array}{l} Cf = \frac{x^2}{\mu \alpha Ra_x} \tau_w \Big|_{y=0}, \tau_w = \mu \frac{\partial u}{\partial y}, \\ Nu = \frac{q_w}{k_f (T_w - T_\infty)} \Big|_{y=0}, q_w = - \left(k_f + \frac{16 \sigma^* T_\infty^3}{3 k^*} \right) \left(\frac{\partial T}{\partial y} \right). \end{array} \right\} \quad (9)$$

Terms in (5) allows us to rewrite the terms in (9) as

$$\left. \begin{aligned} (Ra_x)^{\frac{1}{4}} Cf_x &= f''(0), \\ (Ra_x)^{-\frac{1}{4}} Nu_x &= -\left(1 + \frac{4}{3}R\right)\theta'(0). \end{aligned} \right\}$$

Results and Discussion

The equations (6-7) with the conditions (8) are solved using bvp4c solver, which is a MATLAB in-built function. The numerical results elucidate the profound impact of key parameters on the flow and thermal fields, with clear physical implications. The attenuation of the velocity profile with rising Weissenberg number, as shown in Fig. 2, is a hallmark of viscoelasticity in the Maxwell fluid; the enhanced fluid elasticity introduces a stronger resistance to flow, thereby thickening the momentum boundary layer and decelerating the fluid. Similarly, the decline in velocity with an increasing couple stress parameter (Fig. 3) physically signifies the growing dominance of rotational viscosity and micro-rotational effects, which resist fluid motion. Thermally, the suppression of the temperature profile with a larger thermal relaxation parameter (Fig. 4) is a direct consequence of the Cattaneo-Christov model, where the finite speed of heat propagation prevents thermal disturbances from diffusing instantaneously, leading to a lower temperature distribution within the boundary layer. Conversely, the temperature enhancement with thermal radiation (Fig. 5) is physically attributed to the additional energy influx from radiative heat transfer, which augments the thermal boundary layer and elevates fluid temperatures. These opposing thermal trends underscore the critical balance between non-Fourier heat conduction and radiative effects in high-temperature applications.

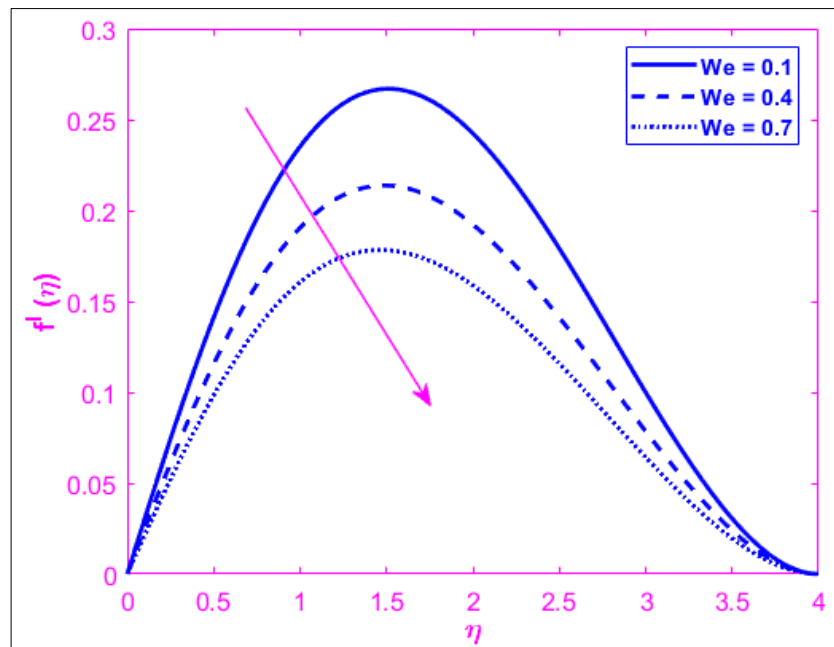


Fig 2: Situation where We influences $f'(\eta)$

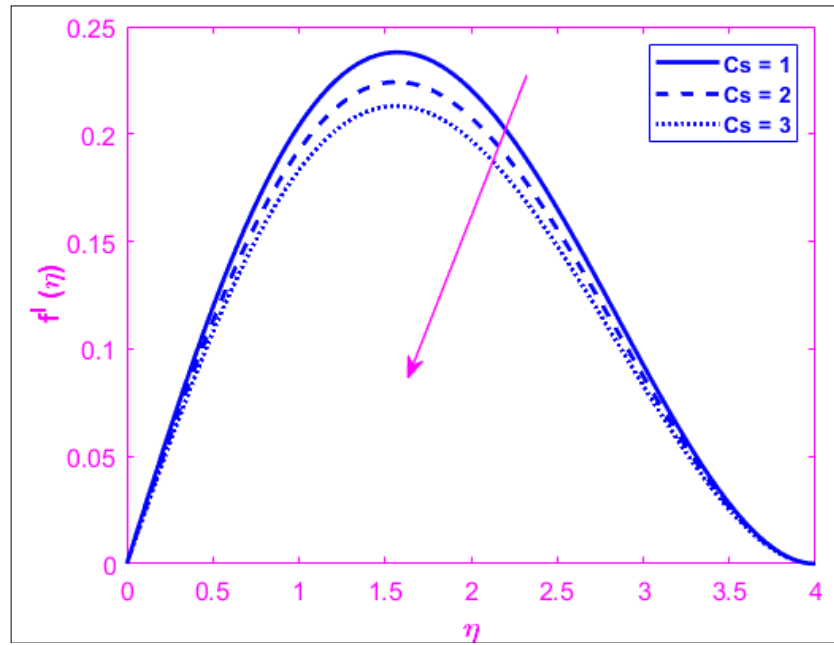
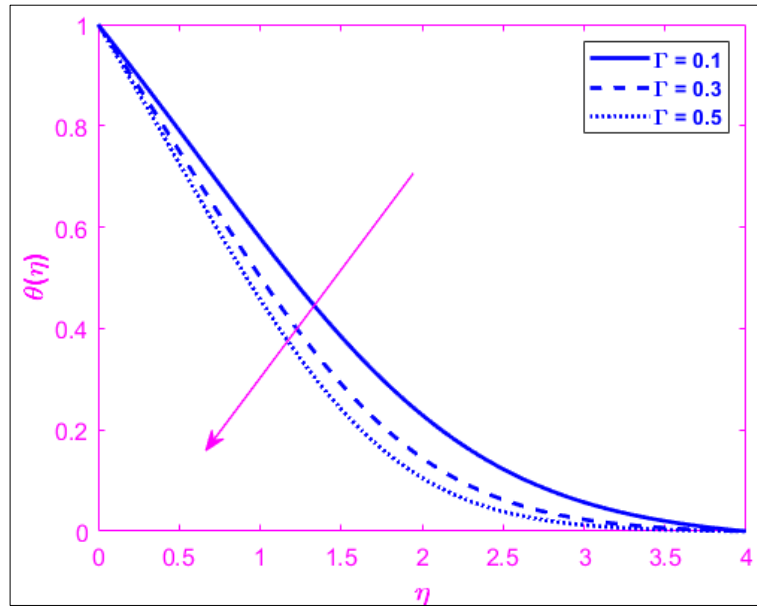
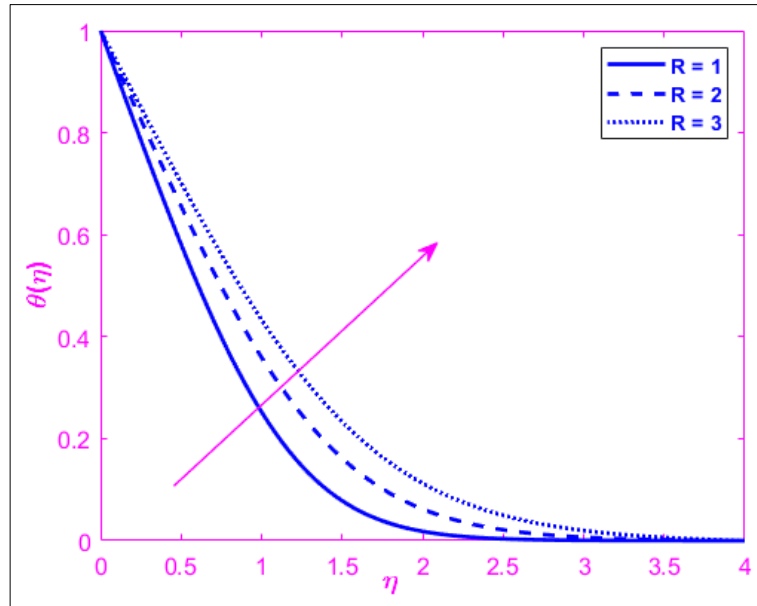


Fig 3: Situation where Cs influences $f'(\eta)$

**Fig 4:** Situation where Γ influences $\theta(\eta)$ **Fig 5:** Situation where R influences $\theta(\eta)$

Multiple linear regression

To translate the numerical findings into practical predictive tools, a multiple linear regression (MLR) analysis was employed. MLR is a statistical technique that models the relationship between a single dependent variable and two or more independent variables by fitting a linear equation to observed data. In engineering design, such models are invaluable for rapidly estimating system performance without resorting to complex, time-consuming simulations. In this study, MLR was used to correlate the influential physical parameters directly with the key engineering quantities of interest: the skin friction coefficient and the Nusselt number. The general forms of the proposed models are:

$$Cf = a_0 + a_1 M + a_2 Cs \quad (10)$$

$$Nu = b_0 + b_1 Pr + b_2 R \quad (11)$$

Utilizing 25 distinct numerical data sets for each correlation, the following specific regression equations were derived:

$$Cf = 0.587 + 0.1578M + 1.5720Cs \quad (12)$$

$$Nu = 0.5421 + 0.4983Pr + 1.2687R \quad (13)$$

The model presented in Equation (12) quantitatively confirms that the skin friction coefficient is an increasing function of both the magnetic field parameter (M) and the couple stress parameter (Cs). The positive coefficients indicate that a stronger magnetic field, which induces resistive Lorentz forces, and increased couple stresses, which enhance rotational viscosity, both contribute to

greater drag at the plate surface. Similarly, Equation (13) demonstrates that the rate of heat transfer, quantified by the Nusselt number, is enhanced by increasing the Prandtl number (Pr) and the thermal radiation parameter (R). A higher Pr signifies a thinner thermal boundary layer relative to the velocity boundary layer, promoting heat conduction, while a larger R injects substantial additional energy via radiation, both mechanisms synergistically boosting thermal performance. These compact regression models provide engineers with efficient and accurate formulae for forecasting hydrodynamic and thermal behaviour in such systems.

Conclusion

This study successfully investigates the significance of non-Fourier heat conduction on the magnetohydrodynamic flow of a Maxwell fluid over an inclined plate. The numerical analysis demonstrates that fluid velocity is impeded by increasing viscoelasticity (Weissenberg number) and micro-rotational effects (couple stress parameter), while the temperature field is significantly influenced by the competing effects of the Cattaneo-Christov heat flux and thermal radiation. The thermal relaxation parameter from the non-Fourier model reduces the temperature profile, whereas thermal radiation enhances it. Furthermore, the application of multiple linear regression yielded robust predictive models, quantitatively establishing that the skin friction coefficient increases with the magnetic field and couple stress, and the Nusselt number is augmented by the Prandtl number and thermal radiation. These findings provide critical insights and practical tools for optimizing thermal management and flow control in relevant industrial processes such as polymer extrusion and advanced solar energy systems.

Table 1: Nomenclature

u, v - Velocity components along and perpendicular to the plate	B - Strength of the applied magnetic field
f - Dimensionless stream function	η - Similarity variable
θ - Dimensionless temperature	We - Weissenberg number
C_s - Couple stress parameter	Γ - Thermal relaxation parameter
R - Thermal radiation parameter	C_f - Skin friction coefficient
Nu - Nusselt number	ρ - Density
Pr - Prandtl number	C_p - Specific heat capacitance

References

1. Kumar MA, Reddy YD, Rao VS, Goud BS. Thermal radiation impact on MHD heat transfer natural convective nanofluid flow over an impulsively started vertical plate. *Case Stud Therm Eng*. 2021;24:100826.
2. Sankad G, Ishwar M, Dhange M. Varying wall temperature and thermal radiation effects on MHD boundary layer liquid flow containing gyrotactic microorganisms. *Partial Differ Equ Appl Math*. 2021;4:100092.
3. Anantha Kumar K, Venkata Ramudu AC, Sugunamma V, Sandeep N. Effect of non-linear thermal radiation on MHD Casson fluid flow past a stretching surface with chemical reaction. *Int J Ambient Energy*. 2022;43(1):8400-8407.
4. Shah SAGA, Hassan A, Karamti H, Alhushaybari A, Eldin SM, Galal AM. Effect of thermal radiation on convective heat transfer in MHD boundary layer Carreau fluid with chemical reaction. *Sci Rep*. 2023;13(1):4117.
5. Bejawada SG, Nandeppanavar MM. Effect of thermal radiation on magnetohydrodynamics heat transfer micropolar fluid flow over a vertical moving porous plate. *Exp Comput Multiph Flow*. 2023;5(2):149-158.
6. Gangadhar K, Prameela M, Chamkha AJ, GR B, Kannan T. Evaluation of homogeneous-heterogeneous chemical response on Maxwell-fluid flow through spiraling disks with nonlinear thermal radiation using numerical and regularized machine learning methods. *Int J Model Simul*. 2024;44:1-23.
7. Sharma K, Kumar L, Singh A, Joshi VK. Hydromagnetic micropolar fluid flow over a stretching sheet under viscous dissipation, thermal radiation and Dufour-Soret effects. *Pramana*. 2024;98(3):119.
8. Mahmood Z, Rehman MU, Rafique K, Adnan, Khan U, Jubair S, *et al*. Time-dependent Casson fluid flow over a vertical Riga plate subjected to slip conditions and thermal radiation: aspects of Buongiorno's model. *Adv Mech Eng*. 2024;16(9):16878132241283290.
9. Omama M, Arafa AA, Elsaied A, Zahra WK. MHD tri-hybrid nanofluid blood flow in a porous cylinder: insights from fractional relaxation modeling with thermal radiation and slip velocity boundary condition. *ZAMM J Appl Math Mech*. 2025;105(1):e202400375.
10. Rafique K, Kanwal S, Niazai S, Alqahtani AA, Khan I. Significance of thermal radiation in stability analysis and triple solutions for magnetized micropolar Buongiorno's nanofluid model. *J Radiat Res Appl Sci*. 2025;18(1):101316.
11. Hayat T, Muhammad K, Alsaedi A. Melting effect and Cattaneo-Christov heat flux in fourth-grade material flow through a Darcy-Forchheimer porous medium. *Appl Math Mech*. 2021;42(12):1787-1798.
12. Tassaddiq A. Impact of Cattaneo-Christov heat flux model on MHD hybrid nano-micropolar fluid flow and heat transfer with viscous and Joule dissipation effects. *Sci Rep*. 2021;11(1):67.
13. Rao DPC, Thiagarajan S, Srinivas Kumar V. Significance of Dufour and Soret effects on the non-Darcy flow of Cross fluid by a tilted plate with radiation and chemical reaction: a Cattaneo-Christov heat flux model. *Heat Transfer*. 2022;51(2):1585-1600.
14. Chandra Sekar Reddy R, Reddy PS, Sreedevi P. Impact of the Cattaneo-Christov heat flux on heat and mass transfer analysis of a hybrid nanofluid flow over a vertical cone. *Int J Ambient Energy*. 2022;43(1):6919-6931.
15. Rehman S, Muhammad N, Alshehri M, Alkarni S, Eldin SM, Shah NA. Analysis of a viscoelastic fluid flow with Cattaneo-Christov heat flux and Soret-Dufour effects. *Case Stud Therm Eng*. 2023;49:103223.
16. Gowda RP, Kumar RN, Kumar R, Prasannakumara BC. Three-dimensional coupled flow and heat transfer in non-Newtonian magnetic nanofluid: an application of Cattaneo-Christov heat flux model. *J Magn Magn Mater*. 2023;567:170329.

17. Ullah R, Israr Ur Rehman M, Hamid A, Arooj S, Khan WA. Heat and mass transport aspect on magnetised Jeffery fluid flow over a stretching cylinder with the Cattaneo-Christov heat flux model. *Mol Phys.* 2024;122(11):e2288701.
18. Khan SU, Adnan, Ramesh K, Riaz A, Awais M, Bhatti MM. Insights into the impact of Cattaneo-Christov heat flux on bioconvective flow in magnetized Reiner-Rivlin nanofluids. *Sep Sci Technol.* 2024;59(10-14):1172-1182.
19. Khattak S, Ahmed M, Abrar MN, Uddin S, Sagheer M, Farooq Javeed M. Numerical simulation of Cattaneo-Christov heat flux model in a porous media past a stretching sheet. *Waves Random Complex Media.* 2025;35(1):1230-1249.
20. Ahmad W, Rehman MIU, Hamid A, Hou M. Heat and mass transfer analysis for thermally radiative Sutterby fluid along a stretching cylinder with Cattaneo-Christov heat flux theory. *J Therm Anal Calorim.* 2025;150(4):2961-2973.
21. Sudarmozhi K, Iranian D, Khan I, Al-johani SA, Eldin SM. Magneto radiative and heat convective flow boundary layer in Maxwell fluid across a porous inclined vertical plate. *Sci Rep.* 2023;13(1):6253.